PROCEEDINGS OF THE NINTH NATIONAL RADIO SCIENCE CONFERENCE FEB. 18-20 , 1992
CAIRO, EGYPT

1 | D3

SPECTRAL DOMAIN ANALYSIS OF SUPERCONDUCTING MICROSTRIP LINES

Abdel-Aziz T. Shalaby*, Emad M. Zieur**, Abdel-Al O. Attia*

* Faculty of Electronic Engineering - Menoufia University, Menouf.

** Institute of Sufficient Productivity - Zagazig University, Zagazig.

Abstract

Spectral domain analysis to calculate the transmission characteristics of low-T_c as well as high-T_c superconducting microstrip lines has been carried out. In this analysis the superconducting film, which is thin compared to its penetration depth, is modeled by an impedance boundary condition. The complex conductivity of the superconductor is described by two models : Mattis-Bardeen equations based on the BCS theory and the two-fluid model. It has been found that the numerical results based on these two models are comparable if an established relationship between them has been used. Numerical results for the propagation constant have been obtained and compared to available experimental data for a low-T_c superconducting microstrip line, and to analytical results for superconducting parallel-plate waveguides.

I. Introduction

New microwave and millimeter wave integrated circuits and components having low loss and low dispersion can be designed using high-T_c ($T_c > 77^{\circ}K$) superconducting thin films [1]. The rapid advances in the processing of the superconducting thin films and substrate materials have made the practical realization of these circuits became possible. To design superconducting microwave elements, such as resonators, filters, and couplers, a knowledge of the transmission characteristics of a superconducting transmission line is required. The transmission of picosecond pulses in a low-T_c ($T_c < 18^{\circ}K$) superconducting coplanar strip line was examined using a closed-form expression for the effective permittivity and BCS modelling for the complex conductivity [2]. Study based on the BCS theory to evaluate the propagation constant of a high-T_c superconducting microstrip line and the substrate effects has been reported [3]. The phenomenological equivalence method [4] in conjunction with the two-fluid model has been used to study the effect of losses in the propagation of pulses on high-T_c superconducting microstrip line [5]. A flexible approach which combines the two-dimensional spectral domain technique and impedance boundary condition has been used to analyze microstrip lines with thin lossy conducting strips. This technique along with the two-fluid model of the complex conductivity has been applied to calculate the transmission characteristics of low-T_c superconducting microstrip lines [6] , [7].

In this paper the spectral domain technique which has been modified to incorporate the impedance boundary condition is applied to calculate the phase and attenuation constants of a high-T_c superconducting microstrip line, $YBa_2Cu_3O_7$ on silicon substrate ($\varepsilon_r = 10.5$). The YBCO superconductor is characterized by critical temperature $T_c = 90^{\circ}K$, and a superconducting energy gap at $T = 0^{\circ}K$ given by $2\Delta(o) \cong 4.5\ K\ T_c \cong 35$ m e.v. [3]. The calculations have been carried out using both of Mattis-Bardeen equations based on the BCS theory and the two-fluid model [8]. Numerical results for the low-T_c superconducting microstrip line, nibbium nitride (NBN) on silicon, have been obtained for the sake of comparison with available experimental data. The NBN superconductor is characterized by a critical temperature $T_c = 12.15^{\circ}K$, and an energy gap at $T = 0^{\circ}K$ given by $2\Delta(o) = 3.52\ K\ T_c \cong$ 3.7 m e.v. [6] , [9]. In all cases, it has been assumed that the thicknesses of the superconducting films are much thinner than the penetration depth, λ.

II. Surface Impedance of a Superconducting Thin Film

The surface Impedance of a plane conductor of arbitrary thickness, t, is given by [10]

$$Z_s = \left(\frac{j\omega\mu_o}{\sigma}\right)^{1/2} \coth\left[\ (j\omega\mu_o\sigma)^{1/2}\ t\ \right] \qquad \ldots\ldots\ldots\ldots\ldots\ldots \quad (1)$$

where σ is the conductivity, and for a normal conductor is a real constant. For a superconductor, σ is a complex quantity and is a function of frequency and temperature. Thus the complex conductivity of a superconductor is given by [8]

$$\sigma = \sigma_1 - j\,\sigma_2 \qquad \ldots\ldots\ldots\ldots\ldots\ldots \quad (2)$$

Expressions for σ_1 and σ_2 based on the two-fluid model and the BCS theory are given in the Appendix. In the case of a superconductor where the thickness is much less than the penetration depth, equation (1) reduces to :

$$Z_s = \frac{1}{\sigma t} = \frac{1}{(\sigma_1 - j\sigma_2)\ t} \qquad \ldots\ldots\ldots\ldots\ldots\ldots \quad (3)$$

Hence, the superconducting thin film can be treated in the electromagnetic field problems as an impedance sheet with a uniform surface impedance, Z_s.

To compare the two-fluid model to Mattis-Bardeen theory the complex conductivity for the NBN superconductor has been calculated using these two theories as shown in Fig. 3. The calculation has been carried out at 1 GHz and as a function of the temperature. The NBN superconductor is characterized by a zero temperature penetration depth (λ_o) of 0.32 μm and a normal state conductivity (σ_n) of $10^6\ (\Omega.m)^{-1}$. These quantities satisfy the following equation which relates the two theories [6]

$$\lambda_o = \left[\frac{h}{\pi\mu_o\sigma_n\,\Delta(o)}\right]^{1/2} \qquad \ldots\ldots\ldots\ldots\ldots\ldots \quad (4)$$

An accurate algorithm to numerically perform the integration in equations (A5) and (A6) has been built. The established program has been checked by comparing the obtained results to those available in the literature [3] for the high-T_c YBCO superconductor. As it is shown in Fig. 3 there is agreement between the two theories in the calculation of the imaginary part of the complex conductivity while this agreement is not present for the real part. However, since $\sigma_2 >> \sigma_1$ in the practical range of operation ($T < T_c$ and $f << f_{gap}$), this disagreement does not affect on the accuracy of the solution. Hence, the two-fluid model adequately predicts the behaviour of the low-T_c as well as high-T_c superconductors as long as λ_o, $\Delta(o)$ and σ_n satisfy equation (4).

III. Formulation

Fig.1 shows a cross-sectional view of a superconducting microstrip line which is assumed to have an electromagnetic wave propagating in the positive $\Im$ direction with a complex propagation constant β. The numerical results of the superconducting microstrip line will be compared to those obtained for a wide superconducting parallel-plate waveguide [11]. Therefore a very large value of the width - to - height ratio, W/d, of the microstrip line is assumed. Under this assumption and to simplify the solution a perfectly conducting ground plane, which is treated as an image plane, is assumed at the plane y = 0. Thus the original microstrip structure is reduced to that shown in Fig. 2 which can be numerically implemented. The propagation constant calculated using this structure has the same value as that of the original structure, but the characteristic impedance differs by a factor of two.

Now, a hybrid-mode analysis based on the spectral domain technique [12] may be applied to derive the complex eigenvalue equation. Following this technique, the field components are expressed in terms of $\bar{E}_y(\alpha_n, y)$ and $\bar{H}y(\alpha_n, y)$ which are the Fourier transforms in the x-direction of the y-field components, $E_y(x,y)$ and $H_y(x,y)$. In these expressions α_n is the discrete transform variable which can be defined for the dominant mode by

$$\alpha_n = (2n + 1)\frac{\pi}{b}, \qquad n = 0, \pm1, \pm2, \pm3, \ldots \qquad \ldots\ldots\ldots\ldots \quad (5)$$

where b is the distance between two assumed perfect electric walls at $x = \pm b/2$ as shown in Fig. 2. This assumption, where b is several times higher than w, makes the infinite Fourier transform in the x-direction discrete transform. Making use of a coordinate transformation, the (x , y , z) into (v , y , u) coordinates, where v is adjusted to the direction of propatgation and y and u are transverse to it, two types of fields will be present. These are TM-to-y ($\bar{E}_y$, $\bar{E}_v$, $\bar{H}_u$) and TE-to-y ($\bar{H}_y$, $\bar{E}_u$, $\bar{H}_v$) fields. Expressions for the wave admittances in the y-direction for the two fields can be derived and are given by [12]

$$Y_{TMi} = \frac{\tilde{H}_u}{\tilde{E}_v} = \frac{j\omega\varepsilon_o\varepsilon_i}{\gamma_i}, \quad Y_{TEi} = -\frac{\tilde{H}_v}{\tilde{E}_u} = \frac{\gamma_i}{j\omega\mu_o}, \; i = 1, 2 \qquad \ldots\ldots\ldots\ldots \quad (6)$$

where, $\gamma_i = \sqrt{\alpha_n^2 + \beta^2 - k_o^2 \varepsilon_i}$ is the complex propagation constant in the y-direction in the i th region. The relations between the surface current density components in the (u,v) coordinates, $J_{sv}(\alpha_n, d/2)$ and $J_{su}(\alpha_n, d/2)$, and the tangential electric fields at the dielectric-air interface, $E_v(\alpha_n, d/2)$ and $E_u(\alpha_n, d/2)$, may be obtained by applying the boundary conditions at the plane $y = d/2$ for the two fields, TM-to-y and TE-to-y. The boundary conditions to be satisfied on the surface of the superconducting thin film are given by [7]

$$\hat{y} \times (E^+ - E^-) = o \qquad \ldots\ldots\ldots\ldots \quad (7a)$$

$$\hat{y} \times (H^+ - H^-) = -\frac{1}{Z_S}\hat{y} \times (\hat{y} \times E^+) = J_S , \qquad \ldots\ldots\ldots\ldots \quad (7b)$$

where the plus and minus sign superscripts refer to field components above and below the sheet, $\hat{y}$ is the unit normal vector, Z_S is the uniform surface impedance of the impedance sheet and J_S is surface current density on the sheet. After applying these boundary conditions we get

$$\tilde{E}_v(\alpha_n) = [\tilde{Z}^e(\alpha_n) - Z_s]\,\tilde{J}_v(\alpha_n) \qquad \ldots\ldots\ldots\ldots \quad (8a)$$

$$\tilde{E}_u(\alpha_n) = [\tilde{Z}^h(\alpha_n) - Z_s]\,\tilde{J}_u(\alpha_n) \qquad \ldots\ldots\ldots\ldots \quad (8b)$$

where,

$$\tilde{Z}^e(\alpha_n) = \frac{1}{\tilde{Y}^e}, \quad \tilde{Y}^e = Y_{TM1} + Y_{TM2}\coth\gamma_2 d \qquad \ldots\ldots\ldots\ldots \quad (9a)$$

$$\tilde{Z}^h(\alpha_n) = \frac{1}{\tilde{Y}^h}, \quad \tilde{Y}^h = Y_{TE1} + Y_{TE2}\coth\gamma_2 d \qquad \ldots\ldots\ldots\ldots \quad (9b)$$

Equations (8) may be transformed to the original (x,z) coordinates to give the following equations

$$[N_x^2\tilde{Z}^e(\alpha_n) + N_3^2\tilde{Z}^h(\alpha_n) - Z_s]\,\tilde{J}_{sx}(\alpha_n) + N_xN_3\,[-\tilde{Z}^e(\alpha_n) + \tilde{Z}^h(\alpha_n)]\,\tilde{J}_{s3}(\alpha_n) = \tilde{E}_x(\alpha_n)$$

$$\ldots\ldots\ldots\ldots \quad (10a)$$

$$N_xN_3\,[-\tilde{Z}^e(\alpha_n) + \tilde{Z}^h(\alpha_n)]\,\tilde{J}_{sx}(\alpha_n) + [N_3^2\tilde{Z}^e(\alpha_n) + N_x^2\tilde{Z}^h(\alpha_n) - Z_s]\,\tilde{J}_{s3}(\alpha_n) = \tilde{E}_3(\alpha_n)$$

$$\ldots\ldots\ldots\ldots \quad (10b)$$

where, $N_x = \alpha_n / \sqrt{\alpha_n^2 + \beta^2}$, $N_3 = \beta / \sqrt{\alpha_n^2 + \beta^2}$.

These equations relate the surface current densities to the tangential electric fields at the plane $y = d/2$ in the (x,z) coordinate system. Applying Galerkin's method in the spectral domain [13] to these equations leads to the following eigenvalue equation in the complex form :

$$F(\beta) = 0 \qquad \ldots\ldots\ldots\ldots \quad (11)$$

In the application of Galerkin's method the surface current densities are expanded in terms of known basis functions as given below, in the space domain,

$$J_{sx}(x) = \sum_{m=1}^{M} a_m J_{xm}(x)\,,\quad J_{sz}(x) = \sum_{m=0}^{N} b_m J_{zm}(x)\,, \qquad \ldots\ldots\ldots\ldots \quad (12)$$

where a_m and b_m are unknown coefficients. The basis functions which have been used here are similar to those used in [6], and are given by

$$\{ J_{xm}(x)\,,\, J_{zm}(x) \} = \frac{\{\sin,\cos\}(2m\pi x / w)}{\sqrt{1-(\frac{2x}{w})^2}} \qquad -\frac{w}{2} < x < \frac{w}{2}$$

$$\ldots\ldots\ldots\ldots \quad (13)$$

$$= \{0,0\} \qquad \text{otherwise}$$

The complex propagation constant, β, may be obtained by solving the complex equation (11). We have built a computer program based on Muller's method for searching the complex root of this equation. In this method information about the starting values to start the iterative process is required. However, for this purpose and for quick prediction closed-form expressions for a superconducting parallel-plate transmission line may be used. These expressions are given by [11]

$$\mathrm{Im}(\beta) = \omega(\mu_o \varepsilon_2)^{1/2}\left[1 + \frac{\lambda}{d}\coth(\frac{t_1}{\lambda}) + \frac{\lambda}{d}\coth(\frac{t_2}{\lambda})\right]^{1/2} \qquad \ldots\ldots\ldots\ldots \quad (14a)$$

$$\mathrm{Re}(\beta) = \frac{(\omega\lambda)^3 \mu_o^2 \varepsilon_2 \sigma_n}{2d\,|\mathrm{Im}(\beta)|}\left[\coth(\frac{t_1}{\lambda}) + \coth(\frac{t_2}{\lambda})\right] \qquad \ldots\ldots\ldots\ldots \quad (14b)$$

where t_1 and t_2 are the thicknesses of the superconducting films.

IV. Numerical Results

Preliminary computations have been carried out to study the convergence of the numerical solution of equation (11) with respect to the number of spectral terms and basis functions. The computations have been carried out on NBN superconducting microstrip line which has NBN ground plane of thickness 150 Å, NBN strip of thickness 140 Å and width 25 μm, and silicon dielectric of thickness 450 Å. The quantity b/w is 4.0. This structure has been chosen to compare the computed results with available experimental measurements [6]. Fig. 4 shows the relative error of the propagation constant (from a reference value : M = N = 5, NS = 5) with respect to the number of the spectral terms at four different values of the expansion of the basis functions (f = 1 Ghz, T = 4°K). As it is shown in the figure, two terms of the expansion of the basis functions and 300 spectral terms are sufficient for very accurate results.

Figs. 5 and 6 show the attenuation and the normalized phase constant (β/k_o), respectively, at 1 GHz as a function of the temperature for the same structure. Also, shown on the same figures results obtaind by equatios (14) at 1GHz for the NBN superconducting parallel-plate line for the sake of comparison. From Fig. 6 it may be noted that there is a good agreement,

better than that obained in [6], between our computed results and the experimental results. Also, from these figures it is clear that the parallel-plate model gives reasonable accuracy for the phase constant but for the attenuation it is not satisfactory.

To compare the low-T_c superconducting microstrip line to that using high-T_c superconductor, again the above structure is considered. Only the NBN superconductor is replaced by the YBCO supperconductor ($\lambda_o = 0.14\ \mu m$, $\sigma_n = 0.5 \times 10^6\ (\Omega.m)^{-1}$ [4]). The attenuation and the normalized phase constant for this structure are shown in Fig. 7 at 1 and 10 GHz. Also, shown on the same figures results for the parallel-plate case at 1 and 10 GHz. As it is clear in Fig. 7 (a) the attenuation strongly depends on the frequency. In the same time the dispersionless behaviour of the superconducting line can be observed in Fig. 7(b) where the curves at 10 GHz overlaped with that of 1 GHz. Finally, we can notice from Figs. 5 and 7(a) that the high-T_c superconducting microstrip line is less attenuation than the low-T_c microstrip line.

V. Conclusion

Full wave analysis to derive the propagation constant of a superconducting microstrip line has been presented. The analysis is valid for both the low-T_c and high-T_c superconductors. The complex conductivitiy of the superconductor has been calculated using the two-fluid model and Mattis-Bardeen theory. Numerical results for the attenuation and the phase shift constant in both of the low-T_c and high-T_c superconducting microstrip lines have been computed and presented. Comparison between the computed results and experimental data for the low-T_c superconducting microstrip line showed very good agreement. The computed resuts have also been compared with those of the parallel-plate waveguide and good agreement has been obtained in the case of the phase shift constant. The high-T_c superconducting microstrip line has shown less attenuation than that of the low-T_c.

Appendix

The complex conductivity of a superconductor is written as

$$\sigma = \sigma_1 - j\sigma_2 \qquad \text{..... (A1)}$$

In the two-fluid model, σ_1 and σ_2 are given by [8]

$$\frac{\sigma_1}{\sigma_n} = \left(\frac{T}{T_c}\right)^4 \qquad \text{..... (A2)}$$

and,

$$\frac{\sigma_2}{\sigma_n} = \frac{1}{\omega\mu_o\sigma_n\lambda^2} \qquad \text{..... (A3)}$$

where,

$$\lambda = \frac{\lambda_o}{\sqrt{1 - \left(\frac{T}{T_c}\right)^4}} \qquad \text{..... (A4)}$$

where σ_n is the normal conductivity near the critical temperature, T_c, and λ_o is the zero temperature penetration depth. Using the BCS theory, Mattis and Bardeen [14] have derived the following expressions for σ_1 and σ_2

$$\frac{\sigma_1}{\sigma_n} = \frac{2}{\hbar\omega}\int_{\Delta}^{\infty} [\,F(E) - F(E+\hbar\omega)\,]\,\frac{E^2+\Delta^2+\hbar\omega E}{(E^2-\Delta^2)^{1/2}\,[\,(E+\hbar\omega)^2-\Delta^2\,]^{1/2}}\,dE \quad \text{.....} \quad (A5)$$

$$+\frac{1}{\hbar\omega}\int_{\Delta}^{\hbar\omega-\Delta} [\,1-2F(\hbar\omega-E)\,]\,\frac{\hbar\omega E - E^2 - \Delta^2}{(E^2-\Delta^2)^{1/2}\,[\hbar\omega-E)^2-\Delta^2\,]^{1/2}}\,dE$$

$$\frac{\sigma_2}{\sigma_n} = \frac{1}{\hbar\omega}\int_{\Delta-\hbar\omega,\,-\Delta}^{\Delta} [\,1-2F(E+\hbar\omega)\,]\,\frac{E^2+\Delta^2+\hbar\omega E}{(\Delta^2-E^2)^{1/2}\,[\,(E+\hbar\omega)^2-\Delta^2\,]^{1/2}}\,dE \quad \text{.....} \quad (A6)$$

where, $F(E) = [\,1+\exp(E/KT)\,]^{-1}$ is the Fermi function, and $\Delta = \Delta(T)$ is the energy gap parameter which may be related to that at zero temperature by the following formula [9]

$$\frac{\Delta(T)}{\Delta(o)} \equiv \sqrt{\cos\left[\frac{\pi}{2}\left(\frac{T}{T_c}\right)^2\right]}\,. \quad \text{.....} \quad (A7)$$

The second integral of σ_1 is zero when $\hbar\omega < 2\Delta$ (or for frequencies below f_{gap}). The lower limit on the integral for σ_2 beomes $-\Delta$ when $\hbar\omega > 2\Delta$.

References

[1] P. A. POLAKOS, C. E. Rice M. V. Schneider and R. Tranbarulo, "Electrical characteristics of thin-film $Ba_2YCu_3O_7$ superonducting ring resonators" IEEE Microwave and Guided Wave Letters, Vol. 1, No. 3, pp. 54 - 56, March 1991.

[2] J. F. Whitaker, R. Sobolewski, D. R. Dykkar, T. Y. Hsiang and G. A. Mourou, "Propagation Model for Ultrafast signals on Superconducting Dispersive Striplines", IEEE Trans. Microwave Theory Tech., Vol. MTT 30, No. 2, PP. 277 - 285, Feb. 1988.

[3] E. B. Ekholm and S. W. McKnight, "Attenuation and Dispersion for High-T_c superconducting Microstrip Lines" IEEE Trans. Microwave Theory Tech., Vol. MTT 38, No. 4, PP. 387 - 395, April 1990.

[4] H. Y., Lee and T., Itoh, "Phenomenological Loss Equivalence Method for Planar Quasi-TEM Transmission Lines with a Thin Normal Conductor or Superconductor, "IEEE Trans. Microwave Theory Tech., Vol. MTT 37, No. 12, PP. 1904 - 909, December 1989.

[5] O. R. Baiocchi, K. Skong, H. Ling and T. Itoh, "Effects of Superconducting Losses in Pulse Propagation on Microstrip Lines" IEEE Microwave and Guided Wave Letters, Vol. 1, No. 1 PP. 2 - 4, June 1991.

[6] J. M. Pond, C. M. Krowne and W. C. Carter, "On the Application of Complex Resistive Boundary Conditions to Model Transmission Lines Consisting of Very Thin Superconductors" IEEE Trans. Microwave Theory Tech., Vol. 37, No. 1, PP. 181 - 190, January 1989.

[7] C. W. Kuo and T. Itoh " A flexible Approach Combining the Spectral Domain Method and impedance Boundary Condition for the Analysis of Microstrip Lines" IEEE Microwave and Guided Wave Letters, Vol. 1, No. 7, PP. 172 - 174, July 1991.

[8] T. Van Duzer and C.W. Turner, "Principles of Superconductive Devices and Circuits", New York, Elsevier, 1981.

[9] J. H. Hinken, Superconductor Electronics - Fundamentals and Microwave Applications, Springer-Verlag, U.S.A., 1989.

[10] E. C. Jordan and K. G. Balmain, Electromagnetic Waves and Radiating Systems, Prentice-Hall, U.S.A., 1968, PP. 153 - 155.

[11] J. C. Swihart, "Field Solution for a thin-film superconducting strip transmission line", J. Appl. Phys., Vol. 32, PP. 461 - 469, March 1961.

[12] T. Itoh, "Spectral Domain Immitance Approach for Dispersion Characteristics of Generalized Printed Transmission lines" IEEE Trans. Microwave Theory Tech., Vo. MTT 28, No. 7, PP. 733 - 736, July 1980.

[13] T. Itoh and R. Mittra, "A Technique for Computing Dispersion Characteristics of Schilded Microstrip Lines" IEEE Trans. Microwave Theory Tech., PP. 896 - 898, October, 1974.

[14] D. C. Mattis and J. Bardeen, "Theory of the anomalous skin effect in normal and superconducting metals" Physl Rev., Vol. III, PP. 412 - 417, 1958.

PROCEEDINGS OF THE NINTH NATIONAL RADIO SCIENCE CONFERENCE FEB. 18-20, 1992 CAIRO, EGYPT

9 D3

URSI

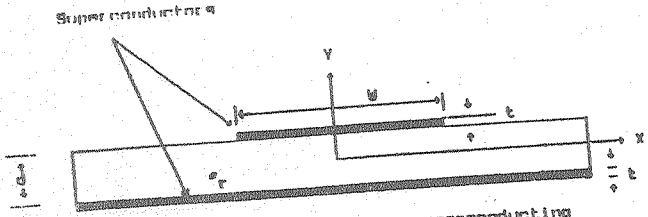

Fig.1 Cross-sectional view of a superconducting microstrip line.

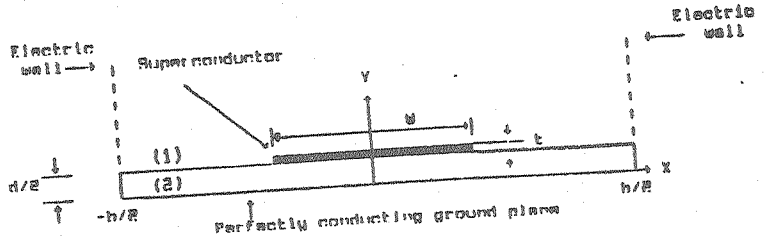

Fig.2 Cross section of superconducting microstrip line backed by a perfectly conducting ground plane.

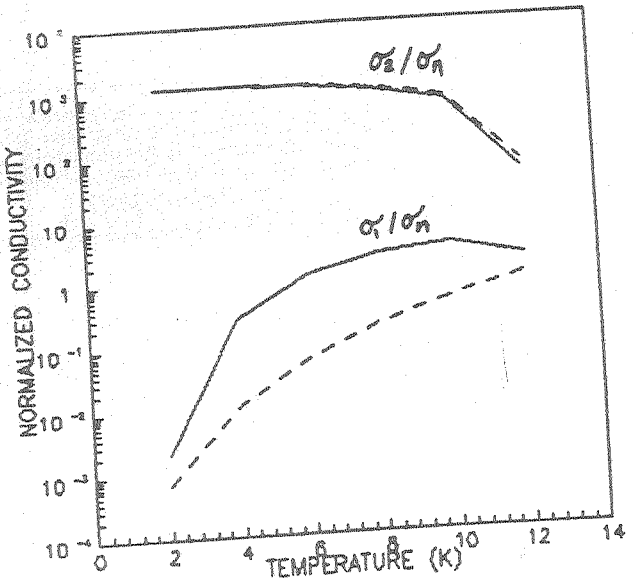

Fig.3 Calculated temperature dependence of the normalized real and imaginary parts of conductivity for a low-Tc NBN superconductor (Tc = 12.15 K) at f =1 GHz using BCS theory (——) and two-fluid model (- - - -).

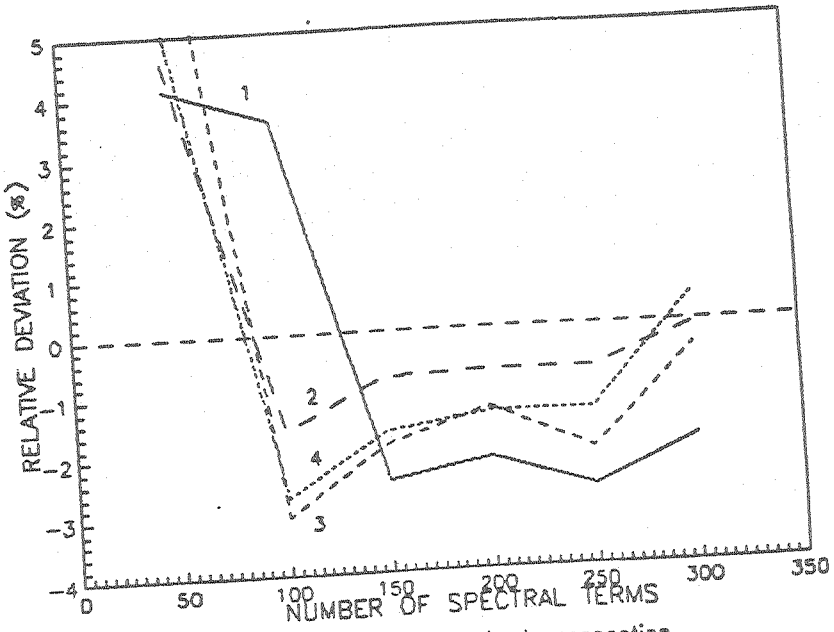

Fig.4. Convergence behavior of the normalized propagation constant as a function of the number of spectral terms NS for different values of the expansion of basis functions ,M=N=1,2,3,4. Reference value:M=N=5,NS=500.

Fig.5 The temperature dependence of the attenuation of the superconducting microstrip line in comparison with that of the superconducting parallel-plate waveguide(_____).

Fig.6 The temperature dependence of the normalized phase constant of the superconducting microstrip line(_____) and that of the parallel-plate waveguide(_____) in comparision with the experimental results(* * *).

(a)

(b)

Fig.7 (a) The attenuation and (b) the normalized phase constant of a high-Tc YBCO superconducting microstrip line(solid curves) and those of parallel-plate case(dashed curves) at 1 and 10 GHz.